A Generalized Sub-Equation Expansion Method and Some Analytical Solutions to the Inhomogeneous Higher-Order Nonlinear Schrödinger Equation

Biao Li[a,c], Yong Chen[a,b], and Yu-Qi Li[a,c]

[a] Nonlinear Science Center, Ningbo University, Ningbo 315211, China
[b] Institute of Theoretical Computing, East China Normal University, Shanghai 200062, China
[c] Key Laboratory of Mathematics Mechanization, Chinese Academy of Sciences, Beijing 100080, China

Reprint requests to Dr. B. L.; E-mail: biaolee2000@yahoo.com.cn

Z. Naturforsch. **63a,** 763 – 777 (2008); received May 5, 2008

On the basis of symbolic computation a generalized sub-equation expansion method is presented for constructing some exact analytical solutions of nonlinear partial differential equations. To illustrate the validity of the method, we investigate the exact analytical solutions of the inhomogeneous high-order nonlinear Schrödinger equation (IHNLSE) including not only the group velocity dispersion, self-phase-modulation, but also various high-order effects, such as the third-order dispersion, self-steepening and self-frequency shift. As a result, a broad class of exact analytical solutions of the IHNLSE are obtained. From our results, many previous solutions of some nonlinear Schrödinger-type equations can be recovered by means of suitable selections of the arbitrary functions and arbitrary constants. With the aid of computer simulation, the abundant structure of bright and dark solitary wave solutions, combined-type solitary wave solutions, dispersion-managed solitary wave solutions, Jacobi elliptic function solutions and Weierstrass elliptic function solutions are shown by some figures.

Key words: Inhomogeneous High-Order NLS Equation; Elliptic Function Solutions; Solitary Wave Solutions.
PACS numbers: 05.45.Yv, 42.65.Tg, 42.81.Dp

1. Introduction

The search for a new mathematical algorithm to discover exact solutions of nonlinear partial differential equations (NLPDEs) is an important and essential task in nonlinear science. Many methods have been developed by mathematicians and physicists to find special solutions of NLPDEs, such as the inverse scattering transformation [1] and Darboux transformation [2], the formal variable separation approach [3], the Jacobi elliptic function method [4], the tanh method [5 – 8], various extended tanh methods [9 – 15], and the generalized projective Riccati equations method [16, 17].

Recently, Fan [18] developed a new algebraic method which further exceeds the applicability of the tanh method in obtaining a series of exact solutions of nonlinear equations. More recently, Yan [19], Chen et al. [20] and Yomba [21] have further developed this method and obtained some new and more general solutions for some NLPDEs.

In this paper, firstly, on the basis of the work done in [5 – 21], we will propose a generalized sub-equation method by a more general ansatz, so that it can be used to obtain more types and general formal solutions, which include a series of nontravelling wave and coefficient function solutions, such as bright-like solitary wave solutions, dark-like solitary wave solutions, W-shaped solitary wave solutions, combined bright and dark solitary wave solutions, single and combined nondegenerate Jacobi elliptic function solutions and Weierstrass elliptic doubly periodic solutions for some NLPDEs. Secondly, to illustrate the validity of the proposed method, we will investigate some exact analytical solutions of the following inhomogeneous higher-order nonlinear Schrödinger equation (IHNLSE) [22], which governs the envelope wave equation for femtosecond optical pulse propagation in inhomogeneous fibers:

$$\begin{aligned} q_z = {} & \mathrm{i}(\alpha_1(z)q_{tt} + \alpha_2(z)|q|^2 q) + \alpha_3(z)q_{ttt} \\ & + \alpha_4(z)(|q|^2 q)_t + \alpha_5(z)q(|q|^2)_t + \Gamma(z)q, \end{aligned} \tag{1}$$

where $q(z,t)$ represents the complex envelope of the electrical field, z is the normalized propagation distance, t is the normalized retarded time, and $\alpha_1(z)$, $\alpha_2(z)$, $\alpha_3(z)$, $\alpha_4(z)$, and $\alpha_5(z)$ are the distributed parameters, which are functions of the propagation distance z, related to the group velocity dispersion (GVD), self-phase-modulation (SPM), third-order dispersion (TOD), self-steepening, and the delayed nonlinear response effect, respectively. $\Gamma(z)$ denotes the amplification or absorption coefficient. The study of the IHNLSE (1) is of great interest due to its wide range of applications. Its use is not only restricted to optical pulse propagation in inhomogeneous fiber media, but also to the core of dispersion-managed solitons and combined managed solitons. In [23], exact multisoliton solutions of (1) are presented by employing the Darboux transformation based on the Lax pair. An exact dark soliton solution of the IHNLSE (1) has been obtained in [24]. When $\Gamma(z) = 0$ in the IHNLSE (1), two exact analytical solutions, that describe the modulation instability and the soliton propagation on a continuous wave background, are obtained by using the Darboux transformation [25]. Using a direct assumption method, Yang et al. [26] presented three exact combined solitary wave solutions for the IHNLSE (1), analyzed the features of the solutions and numerically discussed the stabilities of these solutions under slight violations of the parameter conditions and finite initial perturbations for some exact analytical solutions. Besides the results mentioned above, in recent years, many authors have analyzed the nonlinear Schrödinger-type equation from different points of view and have obtained some interesting and significant results, such as in [27 – 38].

The present paper is organized as follows: In Section 2, the generalized sub-equation expansion method is presented. In Section 3, the proposed method is applied to investigate the IHNLSE (1) and a series of exact analytical solutions of the IHNLSE (1) are obtained. Furthermore some figures are given with computer simulations to show the properties of the kink profile solitary wave solutions, bright-like and dark-like solitary wave solutions, Jacobi elliptic function solutions and Weierstrass elliptic function solutions. Finally, some conclusions are given briefly.

2. The Generalized Sub-Equation Expansion Method

Now we establish the generalized sub-equation expansion method as follows:

Given a NLPDE with, say, two variables $\{z,t\}$:

$$E(u,u_t,u_z,u_{zt},u_{tt},u_{zz},\cdots) = 0. \tag{2}$$

Step 1. We assume that the solutions of (2) are as follows:

$$u(z,t) = \frac{A_0 + \sum_{i=1}^{M} \phi^{i-1}(\xi)\,[A_i\phi(\xi) + B_i\phi'(\xi)]}{a_0 + \sum_{j=1}^{N} \phi^{j-1}(\xi)\,[a_j\phi(\xi) + b_j\phi'(\xi)]}, \tag{3}$$

where $A_0 = A_0(z,t)$, $A_i = A_i(z,t)$, $B_i = B_i(z,t)$ $(i = 1,\cdots,M)$, $a_0 = a_0(z,t)$, $a_j = a_j(z,t)$, $b_j = b_j(z,t)$ $(j = 1,\cdots,N)$, $\xi = \xi(z,t)$ are all differentiable functions of $\{z,t\}$, and the new variable $\phi = \phi(\xi)$ satisfies

$$\phi'^2(\xi) = \left(\frac{\mathrm{d}\phi(\xi)}{\mathrm{d}\xi}\right)^2 = h_0 + h_1\phi(\xi) + h_2\phi^2(\xi) + h_3\phi^3(\xi) + h_4\phi^4(\xi), \tag{4}$$

where h_i $(i = 0,1,2,3,4)$ are constants.

The parameters M and N can be determined by balancing the highest-order derivative term and the nonlinear terms in (2). M,N are usually positive integers; if not, some proper transformation $u(z,t) \to u^m(z,t)$ may be used in order to satisfy this requirement.

Step 2. Substituting (3) along with (4) into (2), extracting the numerator of the obtained system, separating the system into a real and imaginary part, then setting the coefficients of $\phi^i(\xi)(\phi'(\xi))^j$ $(i = 0,1,\cdots;\ j = 0,1)$ to zero, we obtain a set of over-determined PDEs [or ordinary differential equations (ODEs)] with regard to the differential functions A_0, A_i, B_i $(i = 1,2,\cdots,M)$, a_0, a_j, b_j $(j = 1,2,\cdots,N)$, ξ and the varying differential function coefficients included in (2).

Step 3. Solving the overdetermined PDEs (or ODEs) by a symbolic computation system (Maple), we would end up with the explicit expressions for A_0, A_i, B_i $(i = 1,\cdots,M)$, a_0, a_j, b_j $(j = 1,\cdots,N)$, ξ and the functions coefficients or the constraints among them.

Step 4. By using the results obtained in the above steps and the various solutions of (4), a rich set of solutions for (2) can be expected.

By considering the different values of h_0, h_1, h_2, h_3 and h_4, we can derive that (4) admits a series of fundamental solutions. For simplicity, we only list some hyperbolic function solutions, Jacobi elliptic function solutions, and Weierstrass elliptic doubly periodic solutions as follows.

Case 1. If $h_0 = h_1 = 0$, two solutions of (4) are derived:

$$\phi_I^1(\xi) = -4h_2C_0\mathrm{sech}(\sqrt{h_2}\xi)\{2C_0h_3\mathrm{sech}(\sqrt{h_2}\xi) - (\Delta_1+1)\tanh(\sqrt{h_2}\xi) + (\Delta_1-1)\}^{-1}, \tag{5}$$

$$\phi_I^2(\xi) = -4h_2C_0\mathrm{sech}(\sqrt{h_2}\xi)\{2C_0h_3\mathrm{sech}(\sqrt{h_2}\xi) + (\Delta_2+C_0^2)\tanh(\sqrt{h_2}\xi) + (\Delta_2-C_0^2)\}^{-1}, \tag{6}$$

where $h_2 > 0$, $C_0 = \exp(\sqrt{h_2}C_1)$ is an arbitrary constant, and $\Delta_1 = {C_0}^2(4h_2h_4 - {h_3}^2)$, $\Delta_2 = (4h_2h_4 - h_3^2)$.

If further choosing the parameters h_2, h_3, h_4, Δ_1, Δ_2, and C_0 in (5) and (6), we can derive the sech-type solutions

$$\phi_I^3(\xi) = -\frac{h_2}{h_3}\mathrm{sech}^2\left(\frac{\sqrt{h_2}}{2}\xi\right), \quad h_0 = h_1 = h_4 = 0, \quad \Delta_1 = -1 \ (\text{or } \Delta_2 = -C_0^2), \tag{7}$$

$$\phi_I^4(\xi) = \sqrt{-\frac{h_2}{h_4}}\mathrm{sech}\left(\sqrt{h_2}\xi\right), \quad h_0 = h_1 = h_3 = 0, \quad h_4 < 0, \quad \Delta_1 = -1 (\text{or } \Delta_2 = -C_0^2). \tag{8}$$

Case 2. If $h_1 = h_3 = 0$, the Jacobi elliptic function solutions for (4) can be derived:

$$\phi_{II}^1(\xi) = \sqrt{\frac{-h_2m^2}{h_4(2m^2-1)}}\mathrm{cn}\left(\sqrt{\frac{h_2}{2m^2-1}}\xi, m\right), \quad h_4 < 0, \quad h_2 > 0, \quad h_0 = \frac{h_2^2m^2(1-m^2)}{h_4(2m^2-1)^2}, \tag{9}$$

$$\phi_{II}^2(\xi) = \sqrt{\frac{-h_2}{h_4(2-m^2)}}\mathrm{dn}\left(\sqrt{\frac{h_2}{2-m^2}}\xi, m\right), \quad h_4 < 0, \quad h_2 > 0, \quad h_0 = \frac{h_2^2(1-m^2)}{h_4(2-m^2)^2}, \tag{10}$$

$$\phi_{II}^3(\xi) = \sqrt{\frac{-h_2m^2}{h_4(m^2+1)}}\mathrm{sn}\left(\sqrt{-\frac{h_2}{m^2+1}}\xi, m\right), \quad h_4 > 0, \quad h_2 < 0, \quad h_0 = \frac{h_2^2m^2}{h_4(m^2+1)^2}, \tag{11}$$

where $0 \le m \le 1$ is a modulus.

If $m \to 1$ and $m \to 0$, the Jacobi functions degenerate to the hyperbolic functions and the trigonometric functions, respectively, i. e.

$$m \to 1, \quad \mathrm{sn}\xi \to \tanh\xi, \quad \mathrm{cn}\xi \to \mathrm{sech}\xi, \quad \mathrm{dn}\xi \to \mathrm{sech}\xi; \tag{12}$$

$$m \to 0, \quad \mathrm{sn}\xi \to \sin\xi, \quad \mathrm{cn}\xi \to \cos\xi, \quad \mathrm{dn}\xi \to 1. \tag{13}$$

Therefore, when $m \to 1$, the solutions (9) and (10) degenerate to the solution (8), and the solution (11) degenerates to the following solitary wave solution:

$$\phi_{II}^4(\xi) = \sqrt{-\frac{h_2}{2h_4}}\tanh\left(\sqrt{-\frac{h_2}{2}}\xi\right), \quad h_0 = \frac{{h_2}^2}{4h_4}, \quad h_1 = h_3 = 0, \quad h_2 < 0, \quad h_4 > 0. \tag{14}$$

Case 3. If $h_2 = h_4 = 0$, (4) has the following Weierstrass elliptic doubly periodic type solution:

$$\phi_{III}(\xi) = \wp\left(\frac{\sqrt{h_3}}{2}\xi, g_2, g_3\right), \quad \text{where } h_3 > 0, \quad g_2 = -4\frac{h_1}{h_3}, \quad g_3 = -4\frac{h_0}{h_3}. \tag{15}$$

Remark 1. 1) The ansatz (3) presented in this paper is more general than the ansatz by some authors [18 – 21]. (i) When $a_0 = 1$, $a_i = b_i = 0$ $(i = 1,2,\cdots,N)$, A_i, B_i $(i = 0,1,2,\cdots,M)$ are all constants and $\xi = \xi(z,t)$ is only a linear function of $\{z,t\}$, our ansatz in the paper is changed into the ansatz in [18 – 20]. By this ansatz, we only obtain the travelling wave solutions of given PDEs. (ii) When $B_i = 0$ $(i = 1,2,\cdots,M)$, $a_0 = 1$, and $a_j = b_j = 0$ $(j = 1,2,\cdots,N)$, A_i $(i = 0,\cdots,M)$ and ξ are undetermined functions of $\{z,t\}$, the ansatz is changed into the ansatz in [21].

2) Theoretically speaking, one could introduce terms up to 6th, to 8th etc. order or even consider terms of infinite order which might be summed up to give rise to a functionally completely new ansatz. Due to complexity of the computation, the PDEs (or ODEs) systems derived may not be solved in most cases.

3) In order that the PDEs (or ODEs) derived in step 2 can be solved by symbolic computation, we usually choose some special forms of A_i, B_i, a_j, b_j and ξ.

3. Exact Analytical Solutions of the Inhomogeneous Nonlinear Schrödinger Equation

We now investigate the IHNLSE (1) with the generalized sub-equation expansion method of Section 2. According to the method, we assume that the solutions of the IHNLSE (1) are of the special forms

$$q(z,t) = \frac{A_0(z) + A_1(z)\phi(\xi) + B_1(z)\phi'(\xi)}{1 + a_1(z)\phi(\xi) + b_1(z)\phi'(\xi)} \cdot \exp\left\{\mathrm{i}[t^2\lambda_2(z) + t\lambda_1(z) + \lambda_0(z)]\right\}, \tag{16}$$

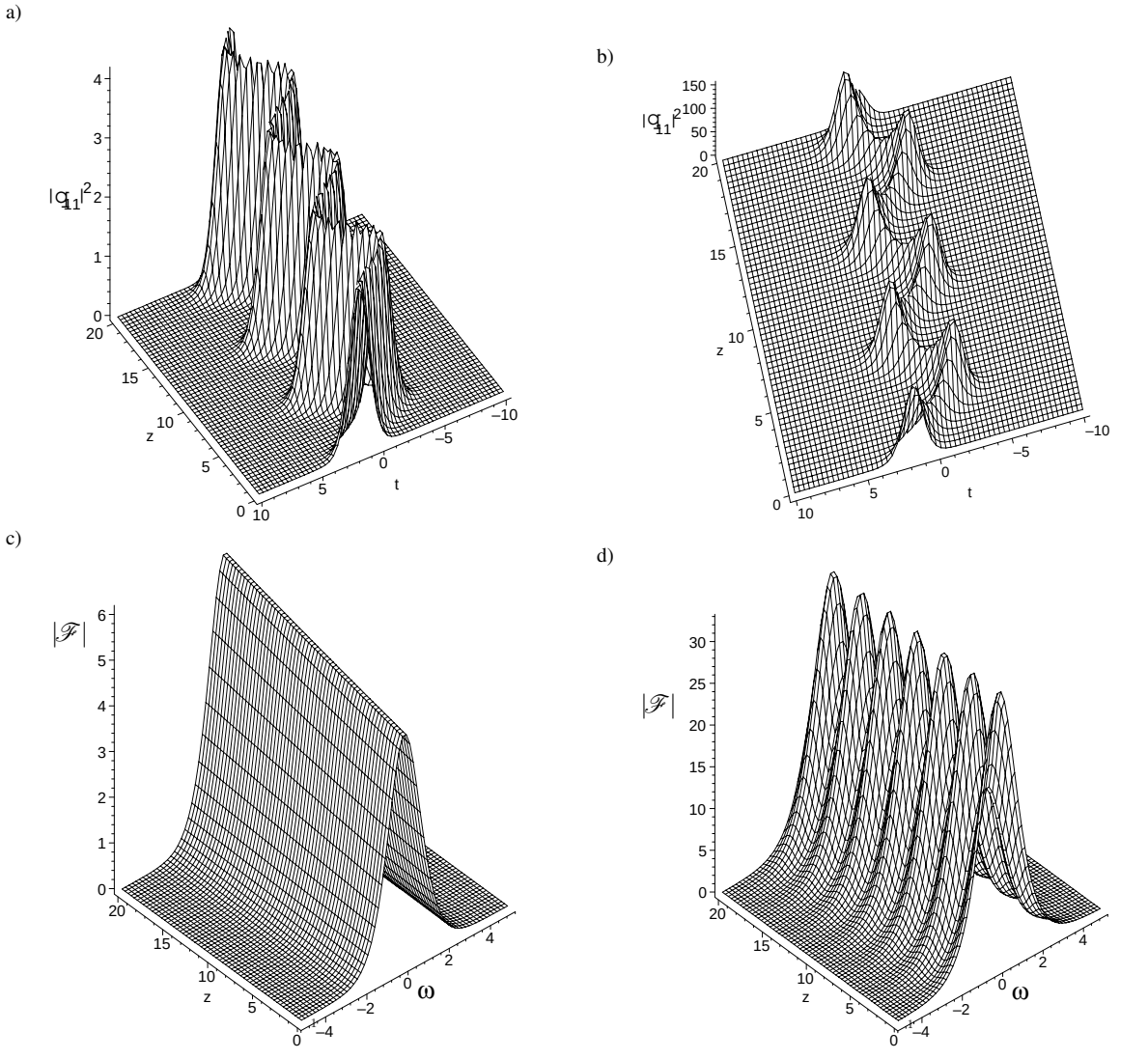

Fig. 1. Evolution plots of the solution (20) with the parameters: $\alpha_1(z) = \alpha_3(z) = \sin(z)$, $h_2 = 2$, $h_3 = -1$, $c_0 = 1$, $c_1 = 1$, $c_2 = 0.1$, $c_4 = 0$, $\mu = 0.1$. (a) $\Gamma(z) = 0.01$; (b) $\Gamma(z) = -0.4\sin(2z)/(1 - 0.4\sin^2 z)$; (c, d) spatial Fourier spectra of the solution (20) corresponding to Fig. 1a and Fig. 1b, respectively.

where

$$\xi = \xi(z,t) = p(z)t + \eta(z), \tag{17}$$

and $A_0(z)$, $A_1(z)$, $B_1(z)$, $a_1(z)$, $b_1(z)$, $\lambda_0(z)$, $\lambda_1(z)$, $\lambda_2(z)$, $p(z)$, and $\eta(z)$ are real functions of z to be determined, and $\phi(\xi)$ satisfies (4).

Substituting (16) and (17) along with (4) into the IHNLSE (1), removing the exponential term, collecting the coefficients of the polynomial of $\phi(\xi)$, $\phi'(\xi)$ and t of the resulting system's numerator, then separating each coefficient into the real part and imaginary part and setting each part to zero, we obtain an ODE system with respect to the differentiable functions $\alpha_1(z)$, $\alpha_2(z)$, $\alpha_3(z)$, $\alpha_4(z)$, $\alpha_5(z)$, $A_0(z)$, $A_1(z)$, $B_1(z)$, $a_1(z)$, $b_1(z)$, $\lambda_0(z)$, $\lambda_1(z)$, $\lambda_2(z)$, $p(z)$, and $\eta(z)$. For simplicity, we omit the ODE system in this paper.

Solving the ODE system with the symbolic computation system Maple, we obtain a rich set of solutions of the system. For simplicity, we omit the too complex and the trivial solutions. Then together with the solutions of the ODE system and (5) – (17), the following

10 families of solutions to the IHNLSE (1) can be derived.

Family 1.

$$q_1(z,t) = \frac{a_1(z)\phi_I(\xi)}{1+\mu\phi_I(\xi)}\exp(\mathrm{i}(c_2 t+\lambda_0(z))), \quad (18)$$

where

$$a_1(z) = c_0\exp\Big[\int \Gamma(z)\mathrm{d}z\Big],\ h_3 = 2\mu h_2,\ h_0 = h_1 = 0,$$

$$\xi = c_1(t+\int (c_1{}^2h_2 - 3c_2{}^2)\alpha_3(z) - 2c_2\alpha_1(z)\mathrm{d}z) + c_4,$$

$$\alpha_5(z) = -\frac{3}{2}\frac{(-2\mu^2h_2+2h_4)c_1{}^2\alpha_3(z)}{(a_1(z))^2} - \frac{3}{2}\alpha_4(z),$$

$$\alpha_2(z) = -\frac{1}{(a_1(z))^2}\big[(-2\mu^2h_2+2h_4)c_1{}^2\alpha_1(z) + (-6c_2\mu^2h_2+6c_2h_4)c_1{}^2\alpha_3(z)\big] - \alpha_4(z)c_2,$$

$$\lambda_0(z) = \int (c_1{}^2h_2 - c_2{}^2)\alpha_1(z) + (3c_1{}^2c_2h_2 - c_2{}^3)\alpha_3(z)\mathrm{d}z + c_3. \quad (19)$$

Here μ, h_2, h_4, c_0, c_1, c_2, c_3, c_4, c_5 are arbitrary constants, and $\alpha_1(z)$, $\alpha_3(z)$, $\alpha_4(z)$, $\Gamma(z)$ are arbitrary functions of z.

If furthermore $h_4 = 0$, from ϕ_I^3 and (18) the following solution of the IHNLSE (1) can be derived:

$$q_{11}(z,t) = \frac{a_1(z)h_2}{-h_3\cosh\left(\frac{\sqrt{h_2}}{2}\xi\right)^2 + \mu h_2}\cdot\exp(\mathrm{i}(c_2t+\lambda_0(z))). \quad (20)$$

In this situation, the solution (20) describes a bright-like solitary wave with the amplitude and the width determined by $a_1(z) = c_0\exp[\int\Gamma(z)\mathrm{d}z]$ and $\sqrt{h_2}c_1/2$, respectively. We note that the time shift $[\chi(z) = -\int(c_1{}^2h_2 - 3c_2{}^2)\alpha_3(z) - 2c_2\alpha_1(z)\mathrm{d}z]$ and the group velocity $[V(z) = \mathrm{d}\chi/\mathrm{d}z = 2c_2\alpha_1(z) - (c_1{}^2h_2 - 3c_2{}^2)\alpha_3(z)]$ of the solitary wave are dependent on z, which leads to a change of the center position of the solitary wave along the propagation direction of the fiber, and means that we may design a fiber system to control the time shift and the velocity of the solitary wave.

In order to understand the evolution of these solutions expressed by (20), let us consider a soliton management system, where the system parameters are trigonometric and hyperbolic functions. For simplicity, we only consider some examples for each solution obtained in Family 1 – 10 under some special parameters.

Figure 1a presents the evolution plots of the solution (20) with $\Gamma(z) = 0.01 > 0$, which corresponds to a dispersion increasing fiber. From it we can see that the intensity of the solitary wave increases when $\Gamma(z) > 0$, and the time shift and the group velocity of the solitary wave are changing while the solitary wave keeps its shape in propagating along the fiber. Figure 1b presents the evolution plots of the solution (20) with $\Gamma(z) = -0.4\sin(2z)/(1-0.4\sin^2 z)$, which corresponds to a fiber, whose dispersion is periodically changing. From it we can see that the intensity of the solitary wave changes periodically, and the time shift and the group velocity of the solitary wave are also changing while the solitary wave keeps its shape in propagating along the fiber. Especially when $\Gamma(z)\to 0$, we can derive that the amplitude of $q_{11}(z,t)$ keeps invariable, unlike in Fig. 1, the amplitude of $q_{11}(z,t)$ either increases exponentially or changes periodically. Figures 1c and 1d are the spatial Fourier spectra of the solution $q_{11}(z,t)$ corresponding to Figs. 1a and 1b, respectively. From the Fourier spectra of the solution $q_{11}(z,t)$, we can derive that the solution $q_{11}(z,t)$ is dominant for low frequencies.

Family 2.

$$q_2(z,t) = c_0\exp\left[\int\Gamma(z)\mathrm{d}z\right](c_1 + c_2\phi_I + c_7\phi_I'(\xi))\cdot\exp(\mathrm{i}(c_4t+c_5)), \quad (21)$$

where

$$\xi = c_3t + c_6,\quad \alpha_1(z) = \alpha_3(z) = 0,\quad \alpha_2(z) = -c_4\alpha_4(z),\quad \alpha_5(z) = -\frac{3}{2}\alpha_4(z), \quad (22)$$

and $h_0 = h_1 = 0$, $c_7 = 0$ (or $c_7 = 1$), and h_2, h_3, h_4, c_0, c_1, c_2, c_3, c_4, c_5, c_6 are arbitrary constants, and $\alpha_4(z)$, $\Gamma(z)$ are arbitrary functions of z.

From ϕ_I^3 and (21), one obtains a solution of the IHNLSE (1) as follows:

$$q_{21}(z,t) = c_0\exp\left[\int\Gamma(z)\mathrm{d}z\right]\cdot\left[c_1 - \frac{h_2}{h_3}\left(c_2 - \sqrt{h_2}\tanh\left(\frac{\sqrt{h_2}}{2}\xi\right)\right)\mathrm{sech}^2\left(\frac{\sqrt{h_2}}{2}\xi\right)\right]\cdot\exp(\mathrm{i}(c_4t+c_5)), \quad (23)$$

where the corresponding parameters are determined by (22) and $c_7 = 1$.

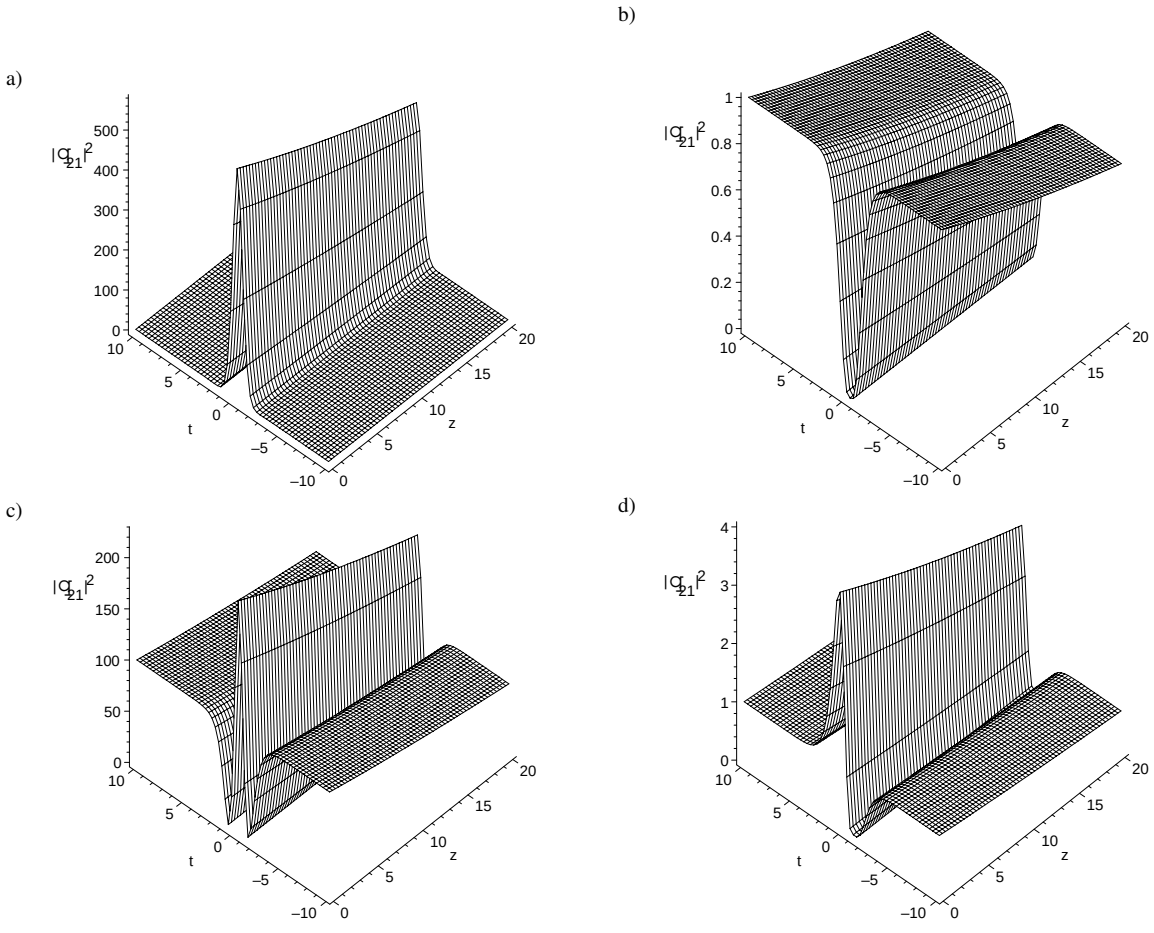

Fig. 2. Evolution plots of the solution (23) with the parameters: $\Gamma(z) = -0.01$, $h_2 = 1$, $c_0 = 1$, $c_3 = 2$, $c_6 = 1$. (a) $h_3 = 0.4$, $c_1 = 1$, $c_2 = 10$; (b) $h_3 = 10$, $c_1 = 1$, $c_2 = 10$; (c) $h_3 = 0.4$, $c_1 = 10$, $c_2 = 10$; (d) $h_3 = 0.4$, $c_1 = 1$, $c_2 = 0.01$.

Because the solution $q_{21}(z,t)$ includes both function $\tanh(\xi)$ and function $\mathrm{sech}(\xi)$, the solution may present different shapes. If $\tanh(\xi)$ [$\mathrm{sech}(\xi)$] is dominant, the solution describes the dark solitary wave (the bright solitary wave). If both effects are nearly equal, the solution presents a combined bright and dark solitary wave. As shown in Fig. 2, under different parameters $\{h_2, h_3, c_1, c_2\}$, the shapes of the intensity (23) take a bright-like solitary wave, dark-like solitary wave, W-shaped solitary wave and a combined bright and dark solitary wave, respectively. It is worth noting that the solitary velocity does not change and there is only a shape-presenting time shift in the propagation due to the constant c_6. In particular, as shown in Fig. 2d, a bright solitary wave and a dark solitary wave are found to combine under some conditions and propagate simultaneously in an inhomogeneous fiber.

Family 3.

$$q_3(z,t) = a_0(z)\left(1 \mp \sqrt{\frac{2h_4}{h_2}}\phi_I\right) \cdot \exp(\mathrm{i}(c_3 t + \lambda_0(z))), \tag{24}$$

where

$$a_0(z) = c_0 \exp\left[\int \Gamma(z)\mathrm{d}z\right],$$

$$h_0 = h_1 = 0, \quad h_3 = \mp 2\frac{h_2 h_4}{\sqrt{h_2 h_4}},$$

$$\xi = c_1 t - \frac{1}{2}c_1 \int 4\alpha_1(z)c_3 + ({c_1}^2 h_2 + 6{c_3}^2)\alpha_3(z)\mathrm{d}z + c_7,$$

$$\alpha_2(z) = -\frac{1}{2(a_0(z))^2}\left[2\alpha_4(z)(a_0(z))^2 c_3 + \alpha_1(z){c_1}^2 h_2 + 3\alpha_3(z){c_1}^2 c_3 h_2 (a_0(z))^2\right],$$

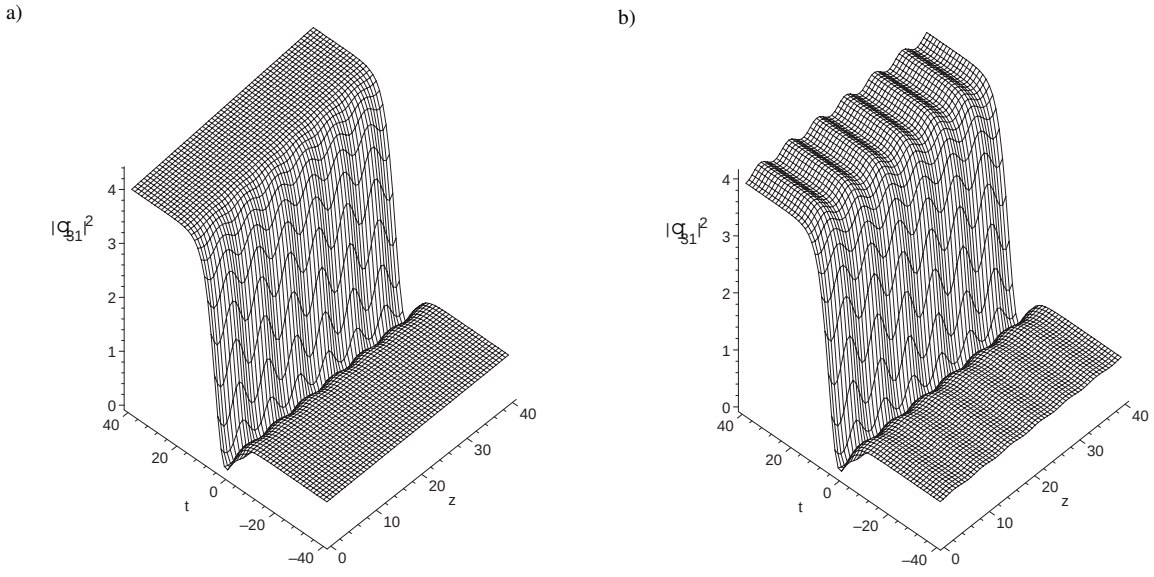

Fig. 3. Evolution plots of the solution (26) with the parameters: $\alpha_1(z)=\alpha_3(z)=\cos(z)$, $h_2=h_4=C_0=1$, $c_0=-2$, $c_1=0.4$, $c_3=0.2$, $c_7=0$. (a) $\Gamma(z)=0.001$; (b) $\Gamma(z)=0.01\sin(z)$.

$$\alpha_5(z)=-\frac{3}{4}\frac{{c_1}^2\alpha_3(z)h_2+2(a_0(z))^2\alpha_4(z)}{(a_0(z))^2},$$

$$\lambda_0(z)=\frac{1}{2}\int(-2{c_3}^2-{c_1}^2h_2)\alpha_1(z) + (-2{c_3}^3-3{c_1}^2c_3h_2)\alpha_3(z)\mathrm{d}z+c_5, \quad (25)$$

and c_0, c_1, c_3, c_5, c_7, h_2, h_4 are arbitrary constants, and $\alpha_1(z)$, $\alpha_4(z)$, $\alpha_3(z)$, $\Gamma(z)$ are arbitrary functions of z.

From $h_3=\mp 2h_2h_4/\sqrt{h_2h_4}$ we obtain $\Delta_1=\Delta_2=0$ in (5) and (6). Thus from (5) and (24) one can obtain a solution for the IHNLSE (1) as follows:

$$q_{31}(z,t)=a_0(z)\big\{1\mp\sqrt{2h_4/h_2}\big[-4h_2C_0\mathrm{sech}(\sqrt{h_2}\xi)\big] \cdot\big[2C_0h_3\mathrm{sech}(\sqrt{h_2}\xi)-\tanh(\sqrt{h_2}\xi)-1\big]^{-1}\big\} \cdot\exp(\mathrm{i}(c_3t+\lambda_0(z))), \quad (26)$$

where the corresponding parameters are determined by (25).

Due to the existence of both function $\tanh(\xi)$ and function $\mathrm{sech}(\xi)$, the solution $q_3(z,t)$ may present different shapes. From Fig. 3 one can see that the intensity of (26) presents mainly kink profile while the solitary wave propagates along the fiber.

Family 4.

$$q_4(z,t)=\frac{a_1(z)(c_1+\phi_I(\xi))}{1+\mu\phi_I(\xi)} \cdot\exp(\mathrm{i}(\lambda_2(z)t^2+c_3\lambda_2(z)t+\lambda_0(z))), \quad (27)$$

where

$$\xi=c_2\lambda_2(z)\left(t+\frac{1}{2}c_3\right)+c_5, \quad h_0=h_1=0,$$

$$\alpha_1(z)=-\frac{1}{4}\frac{\frac{\mathrm{d}}{\mathrm{d}z}\lambda_2(z)}{(\lambda_2(z))^2},\ \alpha_2(z)=\frac{1}{2}\frac{\left(\frac{\mathrm{d}}{\mathrm{d}z}\lambda_2(z)\right){c_2}^2h_4}{(a_1(z))^2(1+\mu c_1)^2},$$

$$h_3=4\frac{c_1h_4}{1+\mu c_1}, \quad h_2=4\frac{{c_1}^2h_4}{(1+\mu c_1)^2},$$

$$\Gamma(z)=\frac{1}{2}\frac{2\lambda_2(z)\frac{\mathrm{d}}{\mathrm{d}z}a_1(z)-a_1(z)\frac{\mathrm{d}}{\mathrm{d}z}\lambda_2(z)}{a_1(z)\lambda_2(z)},$$

$$\lambda_0(z)=\frac{1}{4}\left(c_3^2+\frac{2c_1^2c_2^2h_4}{(1+\mu c_1)^2}\right)\lambda_2(z)+c_4, \quad (28)$$

and $\alpha_3(z)=\alpha_4(z)=\alpha_5(z)=0$, c_1, c_2, c_3, c_4, c_5, h_4, μ are arbitrary constants, and $\lambda_2(z)$, $a_1(z)$ are arbitrary functions of z.

From (28), we can derive that $h_3^2-4h_2h_4=0$. Thus from (8), (27), and (28) a solution of the IHNLSE (1) can be derived:

$$q_{41}(z,t)=\sqrt{\frac{-2h_4\alpha_1(z)}{\alpha_2(z)}}\frac{c_2\lambda_2(z)}{1+\mu c_1}\big[4h_2-2c_1h_3 -c_1C_0(\sinh(\sqrt{h_2}\xi)+\cosh(\sqrt{h_2}\xi))\big]\big[4\mu h_2-2h_3 -C_0(\sinh(\sqrt{h_2}\xi)+\cosh(\sqrt{h_2}\xi))\big]^{-1} \cdot\exp(\mathrm{i}(\lambda_2(z)t^2+c_3\lambda_2(z)t+\lambda_0(z))), \quad (29)$$

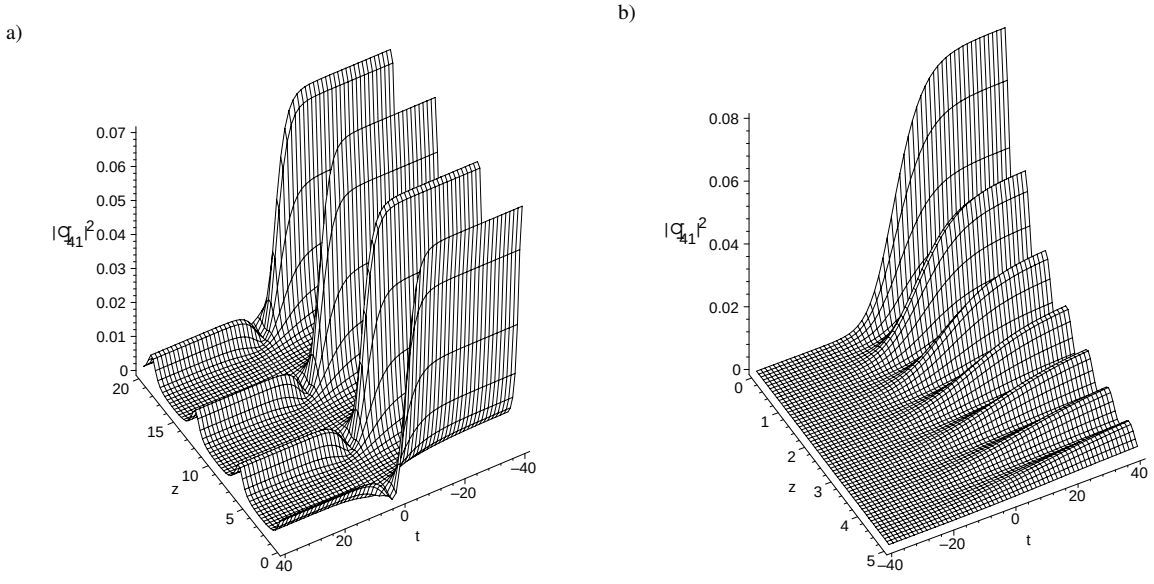

Fig. 4. Evolution plots of the solution (29) with the parameters: (a) $\alpha_1(z)=\sin(z)$, $\alpha_2(z)=-\sin(z)$, $h_2=1$, $h_3=2$, $c_0=6$, $C_0=6$, $c_1=0.1$, $c_2=1$, $c_3=1$, $c_5=0$, $\mu=-2$; (b) $\alpha_1(z)=1-0.8\sin(4z)^2$, $\alpha_2=-1$, $h_2=1$, $h_3=2$, $c_0=5$, $C_0=10$, $c_1=c_2=c_3=1$, $c_5=0$, $\mu=-2$.

where $\alpha_1(z)$ and $\alpha_2(z)$ are arbitrary functions of z, and the corresponding parameters are constrained by

$$\begin{aligned}
&\lambda_2(z)=\frac{1}{\int 4\alpha_1(z)\mathrm{d}z+c_0},\\
&\Gamma(z)=\frac{\alpha_1'(z)\alpha_2(z)-\alpha_1(z)\alpha_2'(z)}{2\alpha_1(z)\alpha_2(z)}-2\alpha_1(z)\lambda_2(z),\\
&\xi=c_2\lambda_2(z)\left(t+\frac{1}{2}c_3\right)+c_5,\\
&h_3=4\frac{c_1h_4}{1+\mu c_1},\quad h_2=4\frac{{c_1}^2h_4}{(1+\mu c_1)^2},\\
&\lambda_0(z)=\frac{1}{4}\left(c_3^2+\frac{2c_1^2c_2^2h_4}{(1+\mu c_1)^2}\right)\lambda_2(z)+c_4.
\end{aligned}\tag{30}$$

Figure 4 presents the evolution plots of the solution (29) under some special parameters. From Fig. 4a one can see that, if the main control functions are $\alpha_1(z)=\sin(z)$, $\alpha_2(z)=-\sin(z)$, the intensity of the solitary wave presents the property of the kink profile solitary wave, and the time shift is changing while the solitary wave keeps its shape in propagating along the fiber. As shown in Fig. 4b, when the main control functions are $\alpha_1(z)=1-0.8\sin(4z)^2$, $\alpha_2=-1$, the intensity of the solution (29) deceases periodically while the kink profile solitary wave propagates along the fiber.

Family 5.

$$\begin{aligned}
q_{51}(z,t)=&\sqrt{\frac{-2\alpha_1(z)h_4}{\alpha_2(z)}}c_1\lambda_2(z)\sqrt{\frac{-h_2m^2}{h_4(2m^2-1)}}\\
&\cdot\mathrm{cn}\left(\sqrt{\frac{h_2}{2m^2-1}}\xi,m\right)\\
&\cdot\exp(\mathrm{i}(\lambda_2(z)t^2+c_2\lambda_2(z)t+\lambda_0(z))),
\end{aligned}\tag{31}$$

$$\begin{aligned}
q_{52}(z,t)=&\sqrt{\frac{-2\alpha_1(z)h_4}{\alpha_2(z)}}c_1\lambda_2(z)\sqrt{\frac{-h_2}{h_4(2-m^2)}}\\
&\cdot\mathrm{dn}\left(\sqrt{\frac{h_2}{2-m^2}}\xi,m\right)\\
&\cdot\exp(\mathrm{i}(\lambda_2(z)t^2+c_2\lambda_2(z)t+\lambda_0(z))),
\end{aligned}\tag{32}$$

$$\begin{aligned}
q_{53}(z,t)=&\sqrt{\frac{-2\alpha_1(z)h_4}{\alpha_2(z)}}c_1\lambda_2(z)\sqrt{\frac{-h_2m^2}{h_4(m^2+1)}}\\
&\cdot\mathrm{sn}\left(\sqrt{-\frac{h_2}{m^2+1}}\xi,m\right)\\
&\cdot\exp(\mathrm{i}(\lambda_2(z)t^2+c_2\lambda_2(z)t+\lambda_0(z))),
\end{aligned}\tag{33}$$

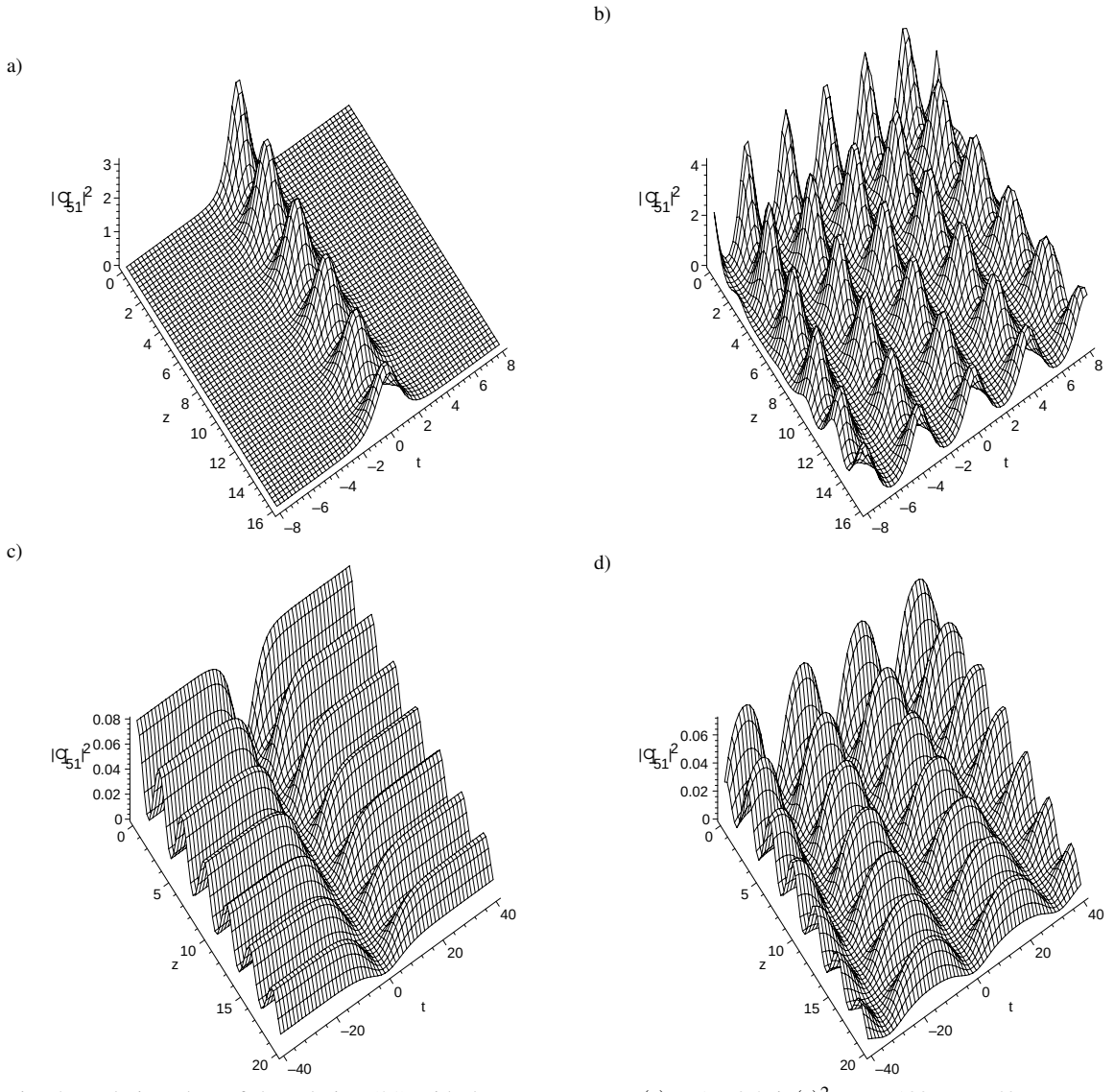

Fig. 5. Evolution plots of the solution (31) with the parameters: $\alpha_1(z) = 1 - 0.8\sin(z)^2$, $c_0 = 100$, $c_1 = 40$, $c_2 = c_4 = 0$. (a, b) $\alpha_2(z) = 1$, $h_2 = 10$, $h_4 = -1$, $m = 1$; (c, d) $\alpha_2(z) = -1$, $h_2 = -0.5$, $h_4 = 1$, $m = 0.9$.

where

$$\xi = c_1\lambda_2(z)\left(t + \frac{1}{2}c_2\right) + c_4, \quad h_1 = h_3 = 0,$$

$$\lambda_0(z) = \frac{1}{4}({c_2}^2 - {c_1}^2 h_2)\lambda_2(z) + c_3,$$

$$\lambda_2(z) = \frac{1}{\int 4\alpha_1(z)\mathrm{d}z + c_0}, \tag{34}$$

$$\Gamma(z) = \frac{\alpha_1'(z)\alpha_2(z) - \alpha_1(z)\alpha_2'(z)}{2\alpha_1(z)\alpha_2(z)} - 2\alpha_1(z)\lambda_2(z),$$

and h_0, h_2, h_4 are constrained by the conditions in $\phi_{II}^1(\xi)$, $\phi_{II}^2(\xi)$ and $\phi_{II}^3(\xi)$, respectively, c_0, c_1, c_2, c_3, c_4 are arbitrary constants, $\alpha_3(z) = \alpha_4(z) = \alpha_5(z) = 0$, $\alpha_1(z)$, and $\alpha_2(z)$ are arbitrary functions of z.

From (12), we can derive that the Jacobi elliptic function solutions $q_{51}(z,t)$, $q_{52}(z,t)$ and $q_{53}(z,t)$ reduce to hyperbolic function solution. At the same time, when $m = 1$, we can conclude that the width, the group velocity and the height of the solitary wave solution $q_{51}(z,t)$ are determined by $\lambda_2(z) = \frac{1}{\int 4\alpha_1(z)\mathrm{d}z + c_0}$, c_2 and

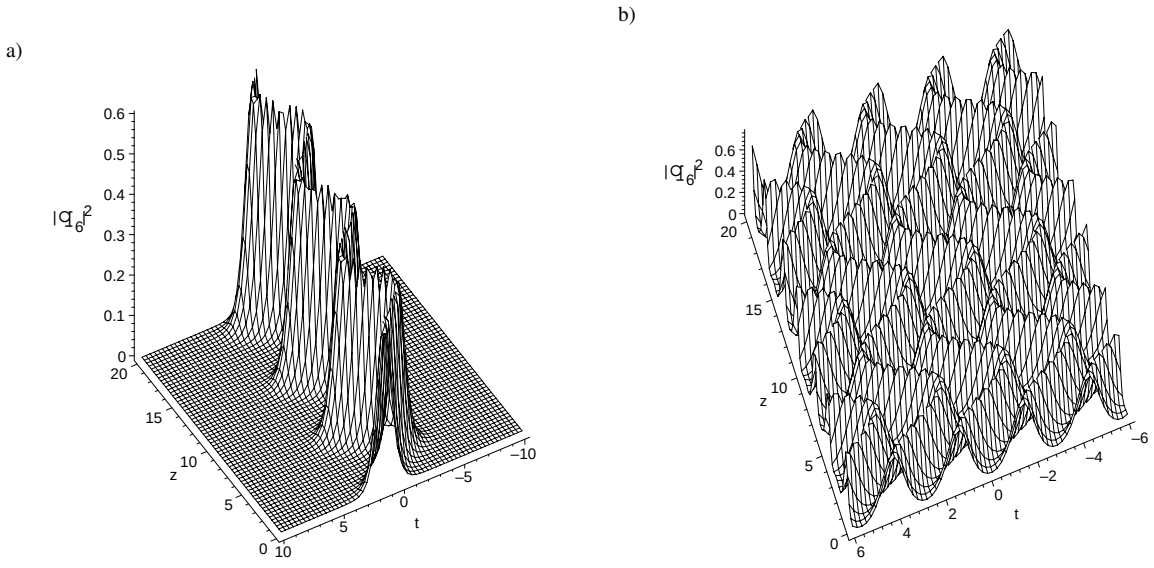

Fig. 6. Evolution plots of the solution (35) of the form $\phi_{II}^1(\xi)$ with the parameters: $\Gamma(z)=0.01$, $\alpha_1(z)=\sin(z)$, $\alpha_3(z)=\sin(z)$, $h_2=0.4$, $h_4=-1$, $c_0=1$, $c_1=2$, $c_2=0.1$, $c_3=c_4=0$. (a) $m=1$; (b) $m=0.9$.

$\sqrt{\frac{-\alpha_1(z)}{\alpha_2(z)}}\lambda_2(z)$, respectively. In essentially, the width and the height are controlled by $\alpha_1(z)$ and $\alpha_2(z)$, the velocity is determined by c_2. Similarly, we can obtain the control functions and control parameters of the solitary wave solution $q_{52}(z,t)$ and $q_{53}(z,t)$ under $m=1$.

The time-space evolution of the dispersion Jacobi elliptic periodic wave solution (31) is shown in Figure 5. From Figs. 5a and 5c, the intensities of the dispersion-managed bright solitary wave and dispersion-managed dark solitary wave are decreasing periodically while the widths of them are increasing in propagating along the fiber. Figures 5b and 5d present the periodic properties of the Jacobi elliptic functions $\mathrm{cn}(\xi,m)$ and $\mathrm{sn}(\xi,m)$.

Family 6.

$$q_6(z,t)=a_1(z)\phi_{II}^i\exp(\mathrm{i}(c_2t+\lambda_0(z))),\ i=1,2,3, \quad (35)$$

where

$$a_1(z)=c_0\exp\left[\int\Gamma(z)\mathrm{d}z\right],$$

$$\xi=c_1\left(t+\int-2c_2\alpha_1(z)+(c_1^2h_2-3c_2^2)\alpha_3(z)\mathrm{d}z\right)+c_4,$$

$$\lambda_0(z)=\int(-{c_2}^2+{c_1}^2h_2)\alpha_1(z)+(-{c_2}^3+3{c_1}^2c_2h_2)\alpha_3(z)\mathrm{d}z+c_3,$$

$$\alpha_2(z)=-\frac{1}{(a_1(z))^2}\left[\alpha_4(z)(a_1(z))^2c_2+2\alpha_1(z){c_1}^2h_4+6{c_1}^2h_4\alpha_3(z)c_2\right],$$

$$\alpha_5(z)=-\frac{3}{2}\frac{2\alpha_3(z){c_1}^2h_4+\alpha_4(z)(a_1(z))^2}{(a_1(z))^2},$$

$$h_1=h_3=0, \quad (36)$$

and h_0, h_2, h_4 are constrained by the conditions in $\phi_{II}^1(\xi)$, $\phi_{II}^2(\xi)$ and $\phi_{II}^3(\xi)$, respectively, c_0, c_1, c_2, c_3, c_4 are arbitrary constants, and $\alpha_1(z)$, $\alpha_3(z)$, $\alpha_4(z)$, $\Gamma(z)$ are arbitrary functions of z.

As shown in Fig. 6, when taking $\phi_{II}^1(\xi)$ in the solution (35), the intensity of the bright-like solitary wave ($m=1$) and the Jacobi elliptic periodic wave ($0<m<1$) are increasing exponentially due to $\Gamma(z)=0.01>0$. If $\alpha_1(z)$ and $\alpha_3(z)$ take trigonometric periodic functions, the time shift and the group velocity of the solitary wave and Jacobi elliptic wave are changing while the waves keeps their shape in propagating along the fiber.

Family 7.

$$q_7(z,t)=c_0\exp\left[\int\Gamma(z)\mathrm{d}z\right]\cdot\left(c_3+c_2\phi_{II}^i(\xi)+c_1(\phi_{II}^i(\xi))'\right)\cdot\exp(\mathrm{i}(c_4t+c_5)),\quad i=1,2,3, \quad (37)$$

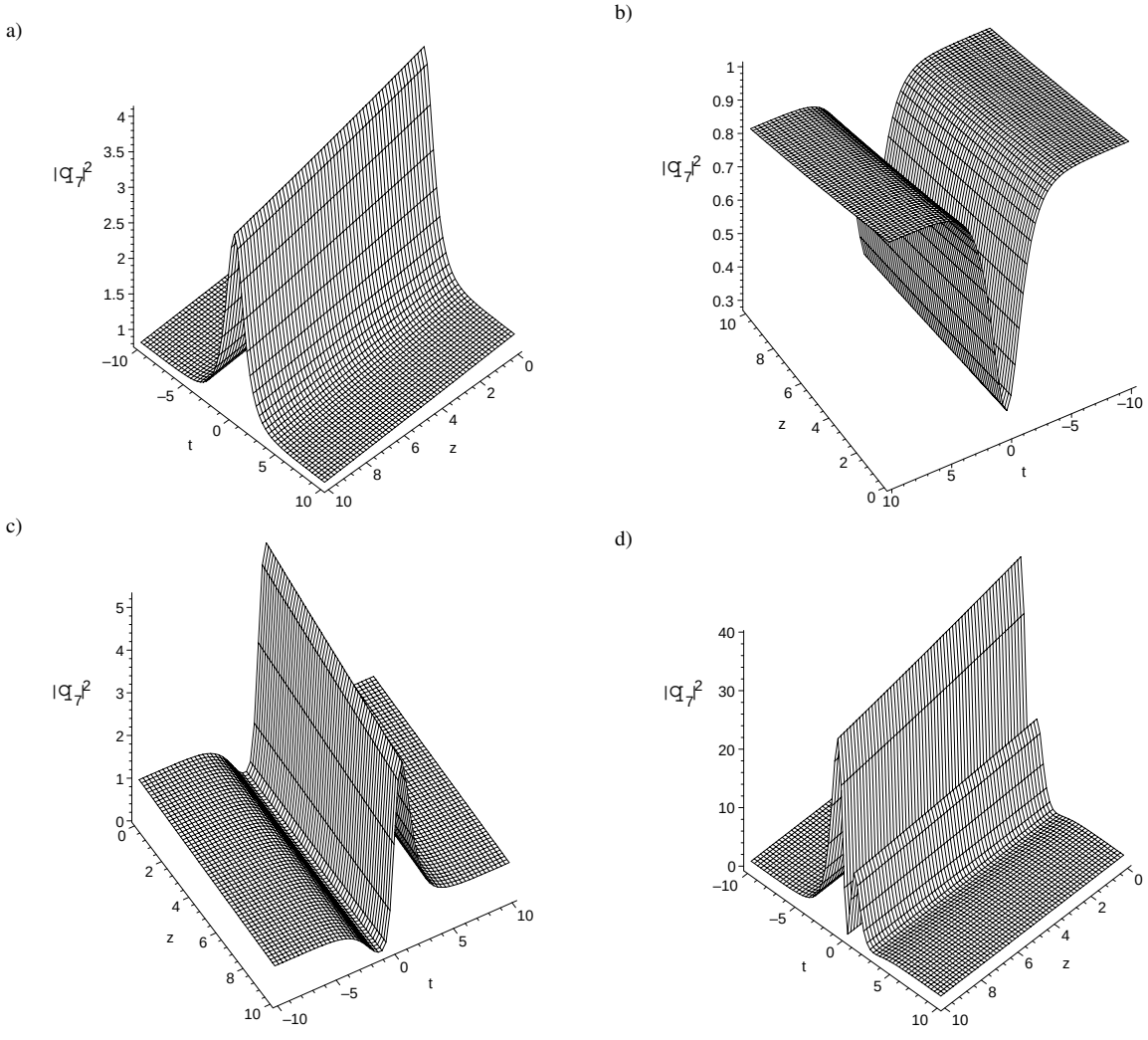

Fig. 7. Evolution plots of the solution (37) with the parameters: $\Gamma(z) = -0.01$, $h_2 = 1$, $h_4 = -1$, $c_0 = c_3 = c_4 = c_5 = m = 1$, $c_6 = 0$. (a) $c_1 = -0.2$, $c_2 = 1$; (b) $c_1 = 0.1$, $c_2 = -0.4$; (c) $c_1 = -2$, $c_2 = 0.4$; (d) $c_1 = 10$, $c_2 = 0.4$.

where

$$\begin{aligned} &\xi = c_3 t + c_6, \quad \alpha_1(z) = \alpha_3(z) = 0, \\ &\alpha_2(z) = -c_4\alpha_4(z), \quad \alpha_5(z) = -\frac{3}{2}\alpha_4(z), \end{aligned} \tag{38}$$

and $h_1 = h_3 = 0$, h_0, h_2, h_4 are constrained by the conditions in $\phi_{II}^1(\xi)$, $\phi_{II}^2(\xi)$ and $\phi_{II}^3(\xi)$, respectively, $c_3 = 0$ (or $c_3 = 1$), c_0, c_1, c_2, c_4, c_5, c_6 are arbitrary constants, and $\alpha_4(z)$, $\Gamma(z)$ are arbitrary functions of z.

As shown in Fig. 7, when taking $\phi_{II}^1(\xi)$ in (35), the shapes of the intensity (35) are determined by c_1 and c_2 under $h_2 = 1$, $h_4 = -1$, $c_3 = m = 1$. A bright-like solitary wave and dark-like solitary wave are shown in Figs. 7a and 7b. In particular, as shown in Figs. 7c and 7d, a bright solitary wave, a dark solitary wave, and two bright solitary waves are found to be combined under some conditions; they propagate simultaneously in an inhomogeneous fiber. It is worth noting that the solitary velocity does not change and there is only a constant time shift in propagation due to constant c_6. At the same time, it is necessary to point out that we only consider some special cases under $m = 1$. If $0 < m < 1$, the evolution of the solutions is similar to Figs. 5 and 6. For simplicity, we do not simulate them in this paper.

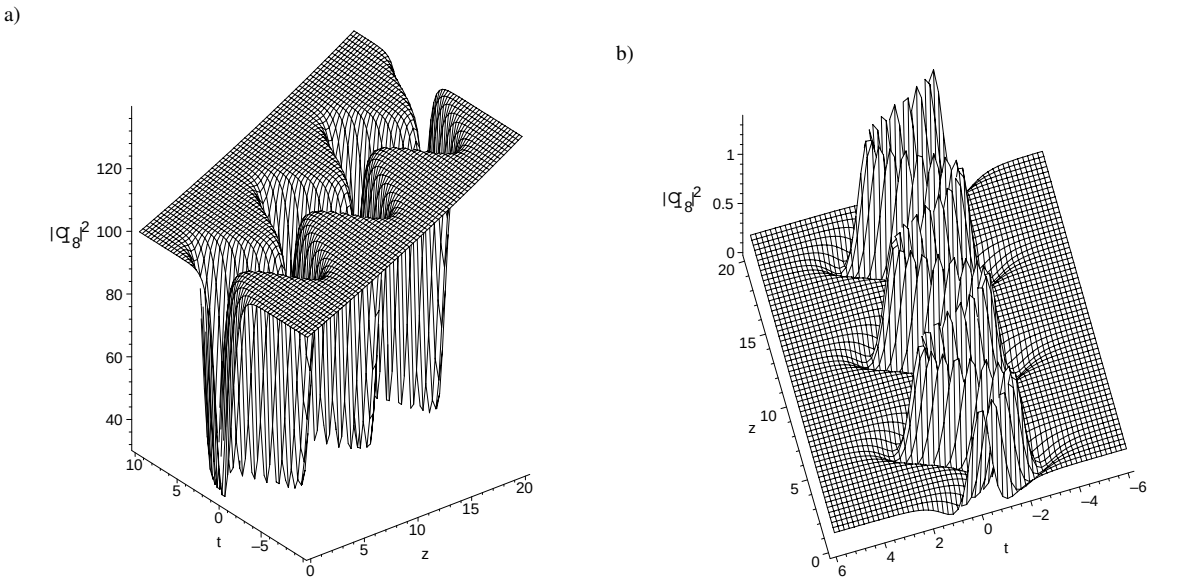

Fig. 8. Evolution plots of the solution (39) of the form $\phi_{II}^1(\xi)$ with the parameters: $\Gamma(z)=0.008$, $\alpha_3(z)=\cos(z)$, $h_2=4$, $h_0=2$, $c_0=c_2=c_3=m=1$, $c_4=c_5=0$, $\mu=3$. (a) $c_1=10$, $h_4=-0.1$; (b) $c_1=-0.4$, $h_4=-1$.

Family 8.

$$q_8(z,t)=\frac{a_1(z)(c_1+\phi_{II}^i(\xi))}{1+\mu\phi_{II}^i(\xi)}\exp(\mathrm{i}(c_3t+\lambda_0(z))),\quad i=1,2,3, \tag{39}$$

where

$$\xi=c_2t-\frac{1}{\mu({c_1}^2\mu^2-1)}\big[(2{c_2}^3\mu^4h_0c_1-2{c_2}^3c_1h_4-3c_2{c_3}^2\mu^3{c_1}^2-4{c_2}^3{c_1}^2h_4\mu+4{c_2}^3\mu^3h_0+3c_2{c_3}^2\mu)\int\alpha_3(z)\mathrm{d}z\big]+c_4,$$

$$\alpha_1(z)=-3\alpha_3(z)c_3,\quad \alpha_2(z)=-\alpha_4(z)c_3,$$

$$\lambda_0(z)=2{c_3}^3\int\alpha_3(z)\mathrm{d}z+c_5,$$

$$\alpha_5(z)=-\frac{3}{2}\alpha_4(z)+3\frac{c_2^2\alpha_3(z)(\mu^4h_0-h_4)}{(a_1(z))^2},$$

$$h_2=-2\frac{\mu^3h_0+c_1h_4}{(c_1\mu+1)\mu},\quad a_1(z)=c_0\exp\left[\int\Gamma(z)\mathrm{d}z\right],$$

$$h_1=h_3=0, \tag{40}$$

and h_0, h_2, h_4 are also constrained by the conditions in $\phi_{II}^1(\xi)$, $\phi_{II}^1(\xi)$ and $\phi_{II}^1(\xi)$, respectively, $\mu\neq0$, c_0, c_1, c_2, c_3, c_4, c_5 are arbitrary constants, and $\alpha_4(z)$, $\Gamma(z)$ are arbitrary functions of z.

As shown in Fig. 8, the intensity of a dark-like solitary wave and a W-shaped solitary wave is increasing exponentially due to $\Gamma(z)=0.01>0$. At the same time, due to the periodicity of the trigonometric periodic functions $\alpha_3(z)$, the time shift and the group velocity of the solitary wave and W-shaped solitary wave are changing while the waves keep their shape in propagating along the fiber.

Family 9.

$$q_9(z,t)=\sqrt{-\frac{10h_0\alpha_1(z)}{\alpha_2(z)}}\mu^2c_1\lambda_2(z)\frac{\wp\left(\frac{\sqrt{h_3}}{2}\xi,\frac{2}{\mu^2},\frac{1}{2\mu^3}\right)}{1+\mu\wp\left(\frac{\sqrt{h_3}}{2}\xi,\frac{2}{\mu^2},\frac{1}{2\mu^3}\right)}\cdot\exp(\mathrm{i}(\lambda_2(z)t^2+c_2\lambda_2(z)t+\lambda_0(z))), \tag{41}$$

where

$$\xi=c_1\lambda_2(z)t+\frac{1}{2}c_1c_2\lambda_2(z)+c_3,\ h_3=-8\mu^3h_0,$$

$$h_1=4\mu h_0,\ h_2=h_4=0,\ \lambda_2(z)=\frac{1}{\int4\alpha_1(z)\mathrm{d}z+c_0},$$

$$\Gamma(z)=\frac{\alpha_1'(z)\alpha_2(z)-\alpha_1(z)\alpha_2'(z)}{2\alpha_1(z)\alpha_2(z)}-2\alpha_1(z)\lambda_2(z),$$

$$\lambda_0(z)=\frac{3}{2}\lambda_2(z)c_1^2\mu^2h_0+\frac{1}{4}c_2^2\lambda_2(z)+c_4,$$

$$\alpha_3(z)=\alpha_4(z)=\alpha_5(z)=0, \tag{42}$$

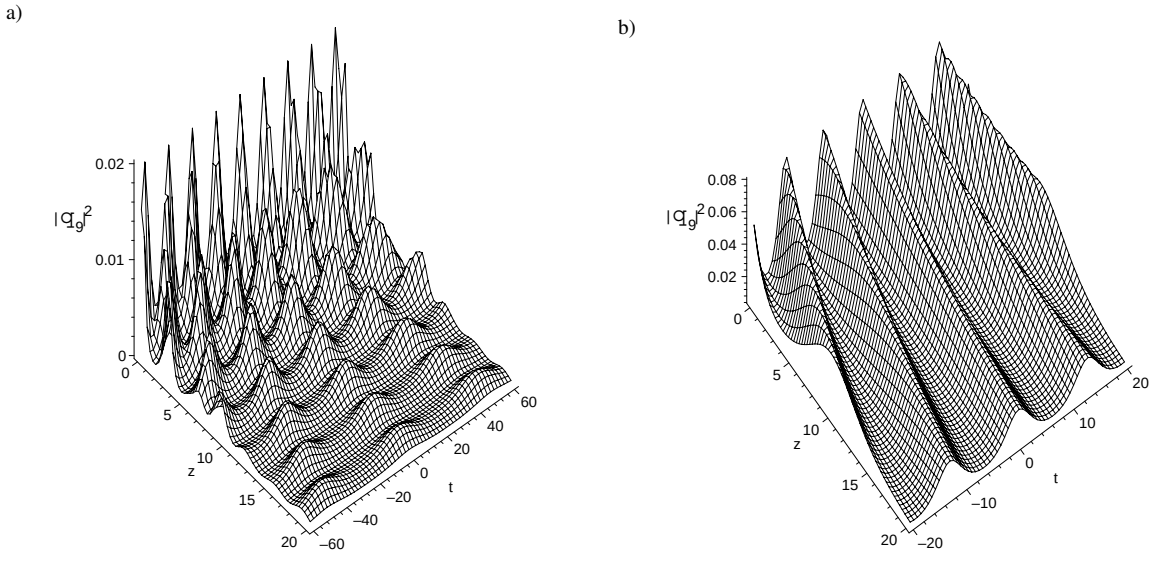

Fig. 9. Evolution plots of the solution (41) with the parameters: (a) $\alpha_1(z) = 1 - 0.8\sin(z)^2$, $\alpha_2(z) = 10$, $h_0 = -1/8$, $c_0 = 20$, $c_1 = 8$, $c_2 = 2$, $c_3 = 0$, $\mu = 1$; (b) $\alpha_1(z) = 0.1$, $\alpha_2(z) = 1$, $h_0 = -1/8$, $c_0 = 10$, $c_1 = 8$, $c_2 = -0.40$, $c_3 = 0$, $\mu = 1$.

and h_0, c_0, c_1, c_2, c_3, c_4 are arbitrary constants, and $\alpha_1(z)$, $\alpha_2(z)$ are arbitrary functions of z.

From Fig. 9 one can see that the evolution of the solution (41) is similar to that shown in Figs. 5b and 5d if the main control functions $\alpha_1(z)$ and $\alpha_2(z)$ are of the same (or similar) forms. As shown in Fig. 9, under the same (or similar) control functions, the evolution of the Weierstrass elliptic doubly periodic type solution (41) is similar to that of the Jacobi elliptic function solution (31).

Family 10.

$$q_{10}(z,t) = c_0 \exp\left[\int \Gamma(z)\mathrm{d}z\right] \frac{\wp\left(\frac{\sqrt{h_3}}{2}\xi, \frac{2}{\mu^2}, \frac{1}{2\mu^3}\right)}{1+\mu\wp\left(\frac{\sqrt{h_3}}{2}\xi, \frac{2}{\mu^2}, \frac{1}{2\mu^3}\right)} \cdot \exp(\mathrm{i}(c_2 t + \lambda_0(z))), \quad (43)$$

where

$$\xi = c_1\left(t - \int (6c_1^2\mu^2 h_0 + 3c_2^2)\alpha_3(z) + 2c_2\alpha_1(z)\mathrm{d}z\right) + c_3,$$

$$h_3 = -8\mu^3 h_0, \quad h_1 = 4\mu h_0, \quad h_2 = h_4 = 0,$$

$$\lambda_0(z) = \int (-6c_1^2\mu^2 h_0 - c_2^2)\alpha_1(z) + (-18\mu^2 c_1^2 c_2 h_0 - c_2^3)\alpha_3(z)\mathrm{d}z + c_4,$$

$$\alpha_2(z) = -\frac{1}{a_1^2(z)}\left[10\mu^4 h_0\alpha_1(z)c_1^2 + \alpha_4(z)a_1^2(z)c_2 + 30\alpha_3(z)c_1^2\mu^4 c_2 h_0\right],$$

$$\alpha_5(z) = -\frac{3}{2}\frac{(a_1^2(z)\alpha_4(z) + 10\alpha_3(z)c_1^2\mu^4 h_0)}{a_1^2(z)},$$

$$a_1(z) = c_0\exp\left[\int \Gamma(z)\mathrm{d}z\right]. \quad (44)$$

Here h_0, c_0, c_1, c_2, c_3, c_4 are arbitrary constants, and $\alpha_1(z)$, $\alpha_2(z)$, $\alpha_3(z)$ are arbitrary functions of z.

From Fig. 10 one can see that the evolution of the solution (43) is similar to that shown in Fig. 6 if the main control functions $\alpha_1(z)$ and $\alpha_2(z)$ are of the same (or similar) forms. Under the same (or similar) control functions, the evolution of the Weierstrass elliptic doubly periodic type solution (41) is similar to that of the Jacobi elliptic function solution (35).

Remark 2. 1) The solutions obtained in the present paper include many previous results by many authors, such as: a) if $c_2 = 0$, $m = 1$, the Theorems 1 and 2 in [27] can be reproduced by our results (31)–(33); b) if $m = 1$, the solutions (51) and (52) in [17] can be also reproduced by (31)–(33); c) if setting $m = 1$ and $\alpha_3(z) = \alpha_4(z) = \alpha_5(z) = 0$ in Family 6, the solutions (48) and (49) in [17] can be recovered. But to our knowledge, the other solutions have not been reported earlier.

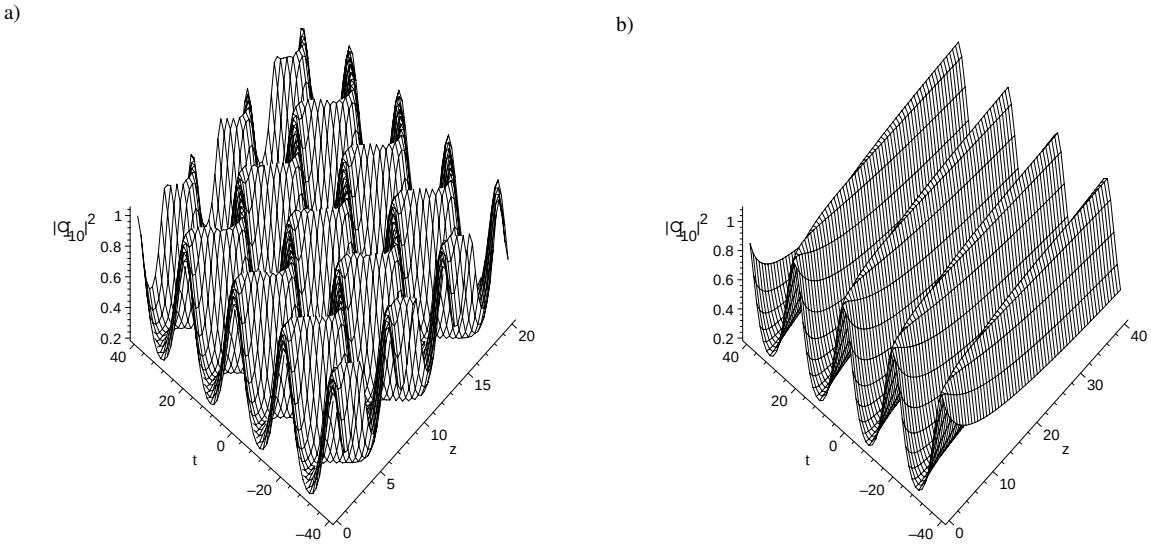

Fig. 10. Evolution plots of the solution (43) with the parameters: $h_0 = -1$, $c_0 = 1$, $c_1 = 0.1$, $c_2 = 1$, $c_3 = c_4 = 0$, $\mu = 1$. (a) $\Gamma(z) = 0.001$, $\alpha_1(z) = \alpha_3(z) = \cos(z)$; (b) $\Gamma(z) = 0.001$, $\alpha_1(z) = \alpha_3(z) = 1/(4z+4)$.

2) The solution presenting the property of the bright solitary wave or dark solitary wave is mainly determined by the function form of the solution. If the solution is only related to the function $\tanh(\xi)$ or $\mathrm{sech}(\xi)$, the solution describes only the dark solitary wave or bright solitary wave, such as $q_{11}(z,t)$, $q_5(z,t)$ and $q_6(z,t)$, each solution presents one form. But if the solution combines function $\tanh(\xi)$ with function $\mathrm{sech}(\xi)$, such as $q_{21}(z,t)$, $q_{31}(z,t)$, $q_{41}(z,t)$, $q_7(z,t)$ and $q_8(z,t)$, the solution may present various shapes, which are determined by whose effect is dominant. If $\tanh(\xi)$ $[\mathrm{sech}(\xi)]$ is dominant, the solution describes the dark solitary wave (the bright solitary wave). If both effects are nearly equal, the solution presents a combined bright and dark solitary wave.

3) Because the solutions obtained contain some arbitrary functions and arbitrary constants, the solutions present abundant structures. As shown in the figures, we found W-shaped solitary waves, combined-type solitary waves, dispersion-managed solitary waves, periodic propagating Jacobi elliptic function waves and Weierstrass elliptic function waves. For simplicity, to each solution, we only considered some special parameter conditions. If taking different parameters in each solution, abundant structures can be expected.

4. Summary and Discussion

In this paper, on the basis of symbolic computation, we presented a generalized sub-equation expansion method to construct some exact analytical solutions of nonlinear partial differential equations. Making use of the method, we investigated several exact analytical solutions of the inhomogeneous high-order nonlinear Schrödinger equation including not only the group velocity dispersion, self-phase-modulation, but also various high-order effects, such as the third-order dispersion, self-steepening and self-frequency shift. As a result, a broad class of exact analytical solutions of the IHNLSE was obtained, which include bright and dark solitary wave solutions, combined-type solitary wave solutions, dispersion-managed solitary wave solutions, Jacobi elliptic function solutions and Weierstrass elliptic function solutions. As shown in the figures produced by computer simulation, these solutions possess abundant structures. From our results, many previous solutions of some nonlinear Schrödinger-type equations can be recovered by means of some suitable choices of the arbitrary functions and arbitrary constants. The method developed provides a systematic way to generate various exact analytical solutions of the IHNLSE with varying coefficients and can be used also for other PDEs. The development of a new mathematical algorithm to discover analytical solutions, especially solitary wave solutions, in nonlinear dispersion systems with spatial parameter variations is important and might have significant impact on future research.

Acknowledgements

The work was supported by NSF of China under Grant Nos. 10747141 and 10735030, Zhejiang Provincial NSF of China under Grant No. 605408, Ningbo NSF under Grant Nos. 2007A610049 and 2006A610093, and K.C. Wong Magna Fund of Ningbo University .

[1] M. J. Ablowitz and P. A. Clarkson, Soliton, Nonlinear Evolution Equations and Inverse Scattering, Cambridge University Press, New York 1991.
[2] C. H. Gu, H. S. Hu, and Z. X. Zhou, Darboux Transformation in Soliton Theory and its Geometric Applications, Shanghai Scientific and Technical Publishers, Shanghai 1999.
[3] S. Y. Lou, Phys. Lett. A **277**, 94 (2000); S. Y. Lou and H. Y. Ruan, J. Phys. A **34**, 305 (2001); X. Y. Tang, S. Y. Lou, and Y. Zhang, Phys. Rev. E **66**, 046601 (2002).
[4] S. K. Liu, Z. T. Fu, S. D. Liu, and Q. Zhao, Phys. Lett. A **289**, 69 (2001).
[5] S. Y. Lou, G. X. Huang, and H. Y. Ruan, J. Phys. A **24**, L587 (1991).
[6] Z. B. Li and Y. P. Liu, Comput. Phys. Commun. **148**, 256 (2002).
[7] W. Malfliet and W. Hereman, Phys. Scr. **54**, 563 (1996).
[8] E. J. Parkes and B. R. Duffy, Comput. Phys. Commun. **98**, 288 (1996).
[9] E. Fan, Phys. Lett. A **277**, 212 (2000); **294**, 26 (2002).
[10] Z. Y. Yan, Phys. Lett. A **292**, 100 (2001); Z. Y. Yan and H. Q. Zhang, Phys. Lett. A **285**, 355 (2001).
[11] Z. S. Lü and H. Q. Zhang, Chaos, Solitons and Fractals **17**, 669 (2003).
[12] B. Li, Y. Chen, and H. Q. Zhang, J. Phys. A **35**, 8253 (2002).
[13] E. Yomba, Chaos, Solitons and Fractals **20**, 1135 (2004); **22**, 321 (2004).
[14] Y. T. Gao and B. Tian, Comput. Phys. Commun. **133**, 158 (2001); B. Tian and Y. T. Gao, Comput. Math. Appl. **45**, 731 (2003).
[15] B. Li, Y. Chen, H. N. Xuan, and H. Q. Zhang, Chaos, Solitons and Fractals **17**, 885 (2003).
[16] B. Li and Y. Chen, Chaos, Solitons and Fractals **21**, 241 (2004); B. Li and H. Q. Zhang, Int. J. Mod. Phys. C **15**, 741 (2004).
[17] B. Li, Z. Naturforsch. **59a**, 919 (2004).
[18] E. Fan, Phys. Lett. A **243**, 243 (2002); J. Phys. A **36**, 7009 (2003); E. Fan and Y. C. Hon, Chaos, Solitons and Fractals **15**, 559 (2003); E. Fan and H. H. Dai, Comput. Phys. Commun. **153**, 17 (2003).
[19] Z. Y. Yan, Chaos, Solitons and Fractals **21**, 1013 (2004).
[20] Y. Chen, Q. Wang, and Y. Z. Lang, Z. Naturforsch. **60a**, 127 (2005).
[21] E. Yomba, Phys. Lett. A **336**, 463 (2005); Chaos, Solitons and Fractals **27**, 187 (2006).
[22] E. Papaioannou, D. J. Frantzeskakis, and K. Hizanidis, IEEE J. Quantum Electron. **32**, 145 (1996).
[23] R. Y. Hao, L. Li, Z. H. Li, and G. S. Zhou, Phys. Rev. E **70**, 066603 (2004).
[24] R. C. Yang, R. Y. Hao, L. Li, Z. H. Li, and G. S. Zhou, Opt. Commun. **242**, 285 (2004).
[25] Z. Y. Xu, L. Li, Z. H. Li, G. S. Zhou, and K. Nakkeeran, Phys. Rev. E **68**, 046605 (2003).
[26] R. C. Yang, L. Li, R. Y. Hao, Z. H. Li, and G. S. Zhou, Phys. Rev. E **71**, 036616 (2005).
[27] V. N. Serkin and A. Hasegawa, Phys. Rev. Lett. **85**, 4502 (2000); V. N. Serkin, T. L. Belyaeva, I. V. Alexandrov, and G. Melo Melchor, Proceedings of SPIE 2001, Vol. 4271, p. 280.
[28] K. Porsezian and K. Nakkeeran, Phys. Rev. Lett. **76**, 3955 (1996).
[29] J. Kim, Q. H. Park, and H. J. Shin, Phys. Rev. E **58**, 6746 (1998).
[30] M. Gedalin, T. C. Scott, and Y. B. Band, Phys. Rev. Lett. **78**, 448 (1997).
[31] S. L. Palacios, A. Guinea, J. M. Fernandez-Diaz, and R. D. Crespo, Phys. Rev. E **60**, R45 (1999).
[32] Z. H. Li, L. Li, H. P. Tian, and G. S. Zhou, Phys. Rev. Lett. **84**, 4096 (2000); Z. H. Li, L. Li, H. P. Tian, G. S. Zhou, and K. H. Spatschek, Phys. Rev. Lett. **89**, 263901 (2002).
[33] W. P. Hong, Opt. Commun. **194**, 217 (2001).
[34] L. Li, Z. H. Li, Z. Y. Xu, G. S. Zhou, and K. H. Spatschek, Phys. Rev. E **66**, 04661 (2002); L. Li, Z. H. Li, S. Q. Li, and G. S. Zhou, Opt. Commun. **234**, 169 (2004).
[35] B. Li, Int. J. Mod. Phys. C **16**, 1225 (2005); B. Li and Y. Chen, Z. Naturforsch. **60a**, 768 (2005); Z. Naturforsch. **61a**, 509 (2006).
[36] M. N. Vinoj, V. C. Kuriakose, and K. Porsezian, Chaos, Solitons and Fractals **12**, 2569 (2001).
[37] K. Nakkeeran, J. Phys. A **34**, 5111 (2001); Phys. Rev. E **62**, 1313 (2000).
[38] R. Ganapathy and V. C. Kuriakose, Chaos, Solitons and Fractals **15**, 99 (2003).